ISSN 2411-3336; e-ISSN 2541-9404

JOURNAL OF MINING INSTITUTE

Zapiski Gornogo instituta

Journal homepage: pmi.spmi.ru

Research article *Geology*

Lamprophyres of the Peshchernoe gold deposit, their geological position, material composition, and metasomatic alterations (Northern Urals)

Dmitrii V. Kuznetsov[1]✉, **Sergei Yu. Stepanov**[2], **Andrei V. Butnyakov**[3], **Viktoriya S. Igosheva**[1]

[1] *The Zavaritsky Institute of Geology and Geochemistry of the Ural Branch of the RAS, Ekaterinburg, Russia*

[2] *South Urals Federal Research Center of Mineralogy and Geoecology of the Urals Branch of the RAS, Ilmenskii State Nature Reserve, Miass, Russia*

[3] *Ural Branch of Polymetal UK, Ekaterinburg, Russia*

How to cite this article: Kuznetsov D.V., Stepanov S.Yu., Butnyakov A.V., Igosheva V.S. Lamprophyres of the Peshchernoe gold deposit, their geological position, material composition, and metasomatic alterations (Northern Urals). Journal of Mining Institute. 2025. Vol. 271. N 16393, p. 22-41.

Abstract

The article presents the first data on biotite-hornblende lamprophyres discovered at the Peshchernoe gold deposit. We consider the geological position of lamprophyre dikes in the deposit structure and the relationship of these rocks with tectonically weakened and mineralized zones. The data on the structural position of mineralized zones, faults, dike bodies, metasomatic halos, and host volcanogenic-sedimentary rocks confirm the tectonic nature of the Peshchernoe deposit alteration system. Lamprophyre dikes are pre-ore, as evidenced by the superimposed metasomatic mineral associations. We assume that dikes of andesitic rocks, lamprophyres, and subsequently hydrothermal fluids, including ore-bearing ones, were intruded along the fault zone of northeastern strike at different geological times. The description of mineralogical and chemical transformations of lamprophyres, which occurred as a result of alteration, is given. Two stages of metasomatism are distinguished: carbon dioxide (beresitization-listvenitization) and subsequent alkaline (sodic metasomatism). During carbon dioxide metasomatism, dark-coloured minerals are replaced by chlorite, albitization and sericitization of plagioclase occur, and ferruginous dolomite is formed under the influence of a significant supply of CO_2. Alkaline (sodic) metasomatism is superimposed on the mineral metasomatic paragenesis of the first stage. We consider metasomatic zoning during sodic metasomatism, manifested in one of the spessartite dikes. Chlorite and relics of magmatic dark-coloured minerals are replaced by magnesite, the supply of Na leads to the appearance of newly formed albite, and the supply of S leads to the formation of pyrite, which concentrates iron from other minerals. As a result of the sodic metasomatism, iron content in carbonates decreases in the direction from the outer metasomatic zone to the inner one. We conclude that it was the alkaline-sulphide sodium solutions that performed the ore-bearing function, and beresitization and listvenitization prepared a favourable environment for ore deposition.

Keywords

gold; Peshchernoe deposit; lamprophyres; beresitization-listvenitization; sodic metasomatism; Krasnoturinskii ore cluster; Northern Urals

Funding

The work was carried out under the state budget-funded research of the Institute of Geology and Geochemistry of the Ural Branch of the RAS (N 123011800009-9); part of the analytical work and field studies were performed at the expense of the state budget-funded research of the South Urals Federal Research Center of Mineralogy and Geoecology of the Urals Branch of the RAS (N 122040600006-1).

Received: 01.03.2023 ***Accepted: 03.06.2024*** ***Online: 30.09.2024*** ***Published:25.02.2025***

Introduction

Dike swarms of various compositions, including lamprophyres, are often present within the ore fields of gold deposits. Lamprophyres are found in gold deposits of various genetic types: orogenic [1, 2], controversial type between orogenic or intrusion-related [3-5], epithermal [6-8], Carlin-type [9-11], reduced intrusion-related RIRGS [12, 13], etc. [14, 15]. Based on frequent spatio-temporal connections between lamprophyres and gold mineralization, it was suggested that they might play a key role in ore formation in mesothermal gold deposits [16-18].

In the Urals, examples of deposits with widespread biotite-hornblende lamprophyre dikes are the Kochkarskoe [19], Berezovskoe [20-22], and Vorontsovskoe [23-25] gold deposits. As a rule, lamprophyre dikes are pre-gold ore [19, 21, 23], as evidenced by the superimposed alteration types. In the case of the Kochkarskoe deposit, most of the gold mineralization occurs in metasomatically altered lamprophyre dikes [19], which have received their own name "tabashki". At the Vorontsovskoe deposit, the gold content in the dikes does not exceed 0.2 g/t [26].

The Peshchernoe deposit is on the eastern slope of the Northern Urals, 4.5 km southwest of the town of Krasnoturinsk. Mineralogically, it belongs to the Krasnoturinsk ore cluster, which includes skarn-magnetite and copper-skarn deposits, as well as the large Vorontsovskoe gold deposit [23, 27]. The deposit area is on the western limb of the Turinskaya brachysyncline, composed of volcanogenic-sedimentary rocks of the Turinskaya Fm. (S_2-D_1*tr*), which have a gentle (10-20°) eastern, northeastern dip (Fig.1, *b*). The Turyinskaya brachysyncline, in turn, is in the eastern part of the Tagil-Magnitogorsk megazone (Fig.1, *a*), in the southern segment of the Auerbakhovskii volcano-plutonic belt, composed of the Late Silurian-Devonian volcanogenic-sedimentary rocks of intermediate composition [28]. 800 m to the east of the deposit is the Poludenskii diorite massif (Fig.1, *c*) of the Early-Middle Devonian gabbro-diorite-granite Auerbakhovskii complex [29]. Small diorite bodies, presumably of the same complex, are present at the deposit.

The Peshchernoe gold deposit was discovered by the Ural Branch of AO Polymetal UK and is currently being mined by ZAO Zoloto Severnogo Urala. The deposit mineralization is classified as gold-low-sulphide-quartz [30]. Volcanogenic-sedimentary rocks in the deposit structure include tuffaceous siltstones and tuffaceous sandstones with interlayers of tuff gritstones, which are intruded by numerous dikes of mafic and intermediate rocks. In terms of chemical composition, tuffaceous siltstones and tuffaceous sandstones correspond to intermediate volcanics of the normal petrochemical series. Gold mineralization is represented by mineralized zones in metasomatically altered volcanogenic-sedimentary rocks (tuffaceous siltstones and tuffaceous sandstones), less often in andesites and basaltic andesites. The most productive ore areas contain minerals of polymetallic paragenesis (pyrite, arsenopyrite, galena, fahlore, chalcopyrite, sphalerite), and gold is found mainly in the form of native segregations, often filling fractures in sulphides.

The position of mineralized zones at the deposit is controlled by northeastern-trending faults occurring subconformably with the contact of volcanogenic-sedimentary rocks of the Turinskaya Fm. and the coeval basalt sequence (Fig.2, *a*, *b*). The faults are accompanied by cataclasis and crushing zones and, according to observations, are marked by lamprophyre dikes. Attitude was measured for several lamprophyre dikes by sampling azimuthally oriented cores. The dip azimuth (d.a.) of the dikes is 120-125° with a dip angle of 55-60°, which is subconformable with the direction and dip angle of the ore zone. The lamprophyre bodies intersect a tuffaceous siltstone sequence, which, according to the bedding (Fig.2, *c*), dips northeast at an angle of 10-15°. Dike thickness ranges from a few tens of centimetres to three metres. Dike contacts and the host tuffaceous siltstones are sharp, with hardening zones to 5 cm thick.

Gold mineralization may have spatial, temporal, structural, paragenetic, or genetic relation to dike complexes. Study of lamprophyres as a component of dike clusters at gold deposits can provide information on the age boundaries of ore formation, the nature and character of metasomatizing fluids, including ore-bearing ones. Since lamprophyres have a consistent mineral and chemical composition, they are more representative for the study of superimposed mineralogical and chemical metasomatic alterations compared to volcanogenic-sedimentary rocks.

Journal of Mining Institute. 2025. Vol. 271. P. 22-41

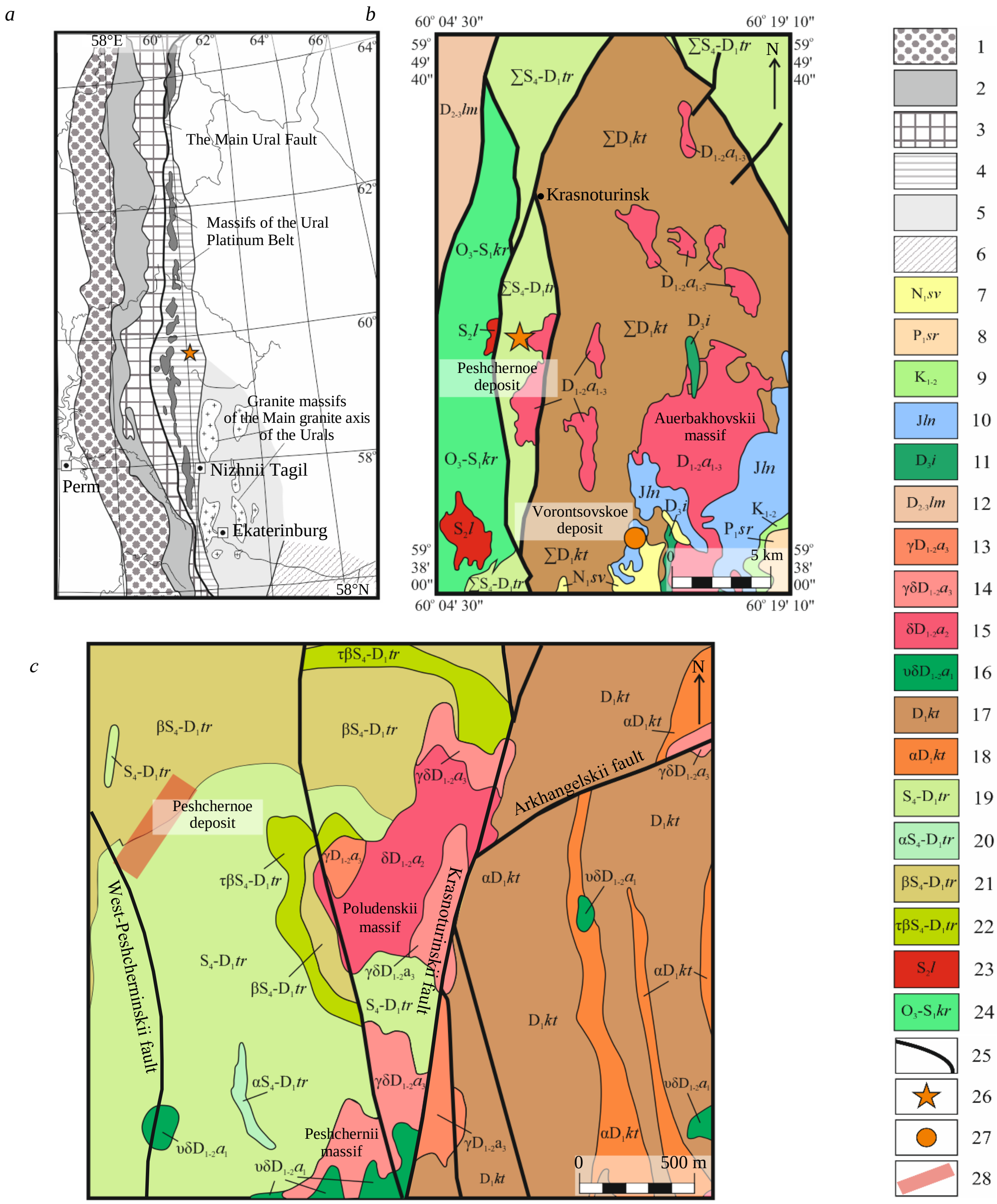

Fig.1. Tectonic zoning of the Middle and Northern Urals (*a*) according to [31], geological map of the Turyinskaya brachysyncline (*b*) and the Peshchernoe deposit area (*c*), compiled based on the report[1] materials and [29, 30] with additions

1 – Cis-Ural foredeep; 2-6 – zones: West Ural (2), Central Ural (3), Tagil-Magnitogorsk (4), East Ural (5), Trans-Ural (6); 7-10 – formations: Svetlinskaya (7), Serovskaya (8), Mysovskaya, Kamyshlovskaya, and Zaikovskaya (9), Langurskaya (10); 11 – gabbrodolerites of the Ivdel complex; 12 – Limkinskaya Fm.; 13-16 – granitoids of the Auerbakhovskii complex ($D_{1-2}a_{1-3}$): granites (13), granodiorites (14), diorites (15), gabbrodiorites and gabbro (16); 17, 18 – rocks of the Krasnoturinskaya Fm. ($\sum D_1 kt$): tuffaceous sandstones and tuffaceous siltstones (17), andesites and their tuffs (18); 19-22 – rocks of the Turinskaya Fm. ($\sum S_4$-$D_1 tr$): tuffaceous sandstones and tuffaceous siltstones (19), andesites and their tuffs (20), basalts and their tuffs (21), trachybasalts and their tuffs (22); 23 – granitoids of the Levinskii complex; 24 – Krasnouralskaya Fm.; 25 – faults; 26 – Peshchernoe deposit; 27 – Vorontsovskoe deposit; 28 – Peshchernoe deposit area

[1] Report of the Serov geological survey party on extensive additional geological study at 1:50,000 scale of the Serov prospect within sheets O-41-1-A (eastern half), O-41-1-B (western half), O-41-1-V, O-41-1-G (western half), O-41-13-A, O-41-13-B (north-western quarter), O-41-13-V, conducted in 1974-1978.

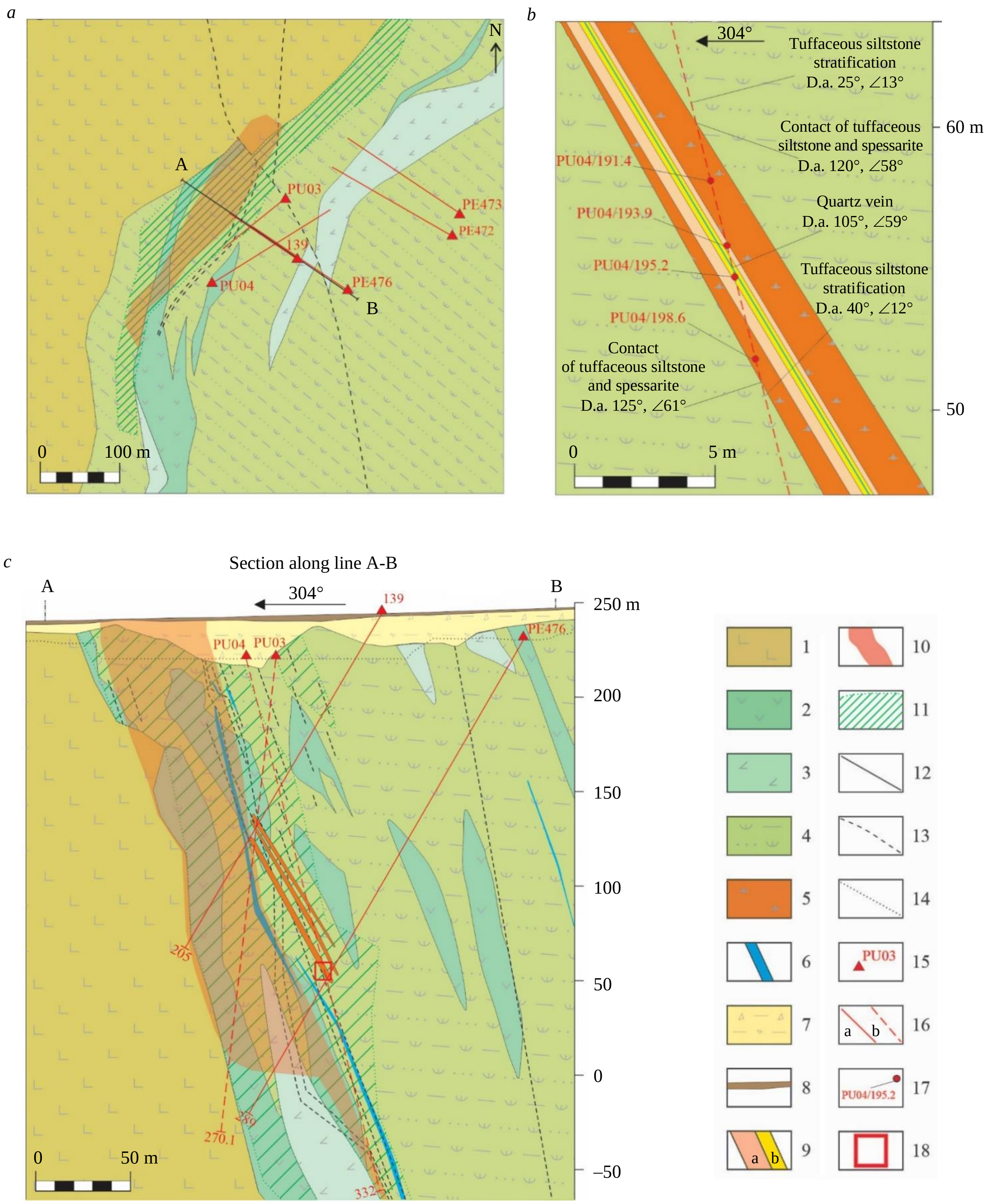

Fig.2. Sketch geological map (*a*) and section (*b*, *c*) of the Peshchernoe deposit
(based on materials from OOO Krasnoturinsk-Polymetal with additions)

1 – basalts; 2 – andesites; 3 – andesibasalts; 4 – tuffaceous siltstones; 5 – spessartites; 6 – quartz veins; 7 – weathering crust; 8 – deluvial deposits; 9 – transition (a) and inner (b) metasomatic zones in a spessartite dike; 10 – ore zone; 11 – metasomatic alterations; 12 – geological boundaries; 13 – tectonic faults; 14 – lower boundary of the quarry at the time of drilling exploratory wells in 2022; 15 – exploratory wells; 16 – projections of exploratory well axes in the section plane (a) and across (b); 17 – sampling points (PU04/191.4 – dike margin, hanging wall, outer metasomatic zone; PU04/193.9 – transition metasomatic zone; PU04/195.2 – dike central part, inner metasomatic zone; PU04/198.6 – dike margin, footwall, outer metasomatic zone); 18 – section area shown at an enlarged scale in Fig.2, *b*

Research methods and materials

The material composition of lamprophyres was studied on samples from several dikes selected from the core of exploratory wells. Their location is indicated in the sketch geological map of the deposit (Fig.2, *a*). The first part of the sample number corresponds to the designation of the exploratory well, and the second, to the sampling depth. The composition of minerals was determined in polished sections on a TESCAN Mira LMS scanning electron microscope using an EDS detector at the Geoanalytic Collective Use Centre of the IGG UB RAS, Ekaterinburg. The following setups were used for surveying: accelerating voltage of 20 kV, electron beam current of 0.8 nA, beam diameter of 8-9 nm. The contents of petrogenic components in rocks were determined by X-ray fluorescence analysis on an SRM-35 multichannel spectrometer. The detection limits for the main part of petrogenic components using this method are in the range of 0.006-0.09 wt.%. The microelement composition of rocks was studied by the ICP-MS method on an Agilent 7700x mass spectrometer at the South Urals Federal Research Center of Mineralogy and Geoecology of the Urals Branch of the RAS, Miass. Thermal analysis was performed on a Diamond TG-DTA thermal analyser and semi-quantitative X-ray phase analysis on an XRD-7000 X-ray diffractometer at the Geoanalyst Collective Use Centre. Gold contents were determined for several samples by atomic absorption spectrometry with electrothermal atomization on a ContrAA 700 spectrometer. The gold detection limit was 0.8 mg/t, and the error did not exceed 40 rel.%.

Research results

Petrographic and mineralogical characteristics of rocks. The rocks of the studied dikes have a dark grey colour, massive texture, porphyritic, lamprophyre, and ocellar structures. Almost all the lamprophyres that make up the dikes are metasomatically altered to varying degrees, which is expressed in the replacement of intermediate plagioclase by albite, the development of dolomite, chlorite, and sericite. Of the preserved primary (magmatic) mineral paragenesis, amphibole, biotite and plagioclase relics are present in the rocks. According to the set of preserved primary minerals, as well as textural and structural features, lamprophyres of the Peshchernoe deposit correspond to spessartites and kersantites [18]. Porphyritic phenocrysts in spessartites are represented by amphibole (Fig.3, *b*, *c*), and in kersantites – by biotite, which is replaced by a mineral aggregate of chlorite and sericite (Fig.3, *a*). Ocelli have a rounded shape, 1-2 mm in size, and are composed of an aggregate of dolomite, quartz, and albite (Fig.3, *c*). The rock bulk consists of plagioclase, dolomite, quartz, chlorite, and sericite. The pyrite content in the studied samples varies from 0.5 to 5 vol.%. Sphalerite, pentlandite, and chalcopyrite are present in pyrite as small inclusions. Monazite, apatite, rutile, and chrome spinelide were found among the accessory minerals.

In the central part of one of the spessartite dikes there is a fracture filled with quartz, probably marking the permeability zone. Along the well axis the thickness of this dike was 12.2 m, with a true thickness of 3.1 m (see Fig.2, *c*). The fracture dip azimuth is 105°, with a dip angle of 60°, which is subconformable with the dip direction of the dike itself. From the permeable zone towards the edge of the dike there are several zones of metasomatic alterations: inner, transition, and outer. The boundaries between the metasomatic zones are distinct. Sometimes quartz veinlets 1-2 mm thick run along them. The rock in the outer metasomatic zone is dark grey. The mineral composition is similar to that of metasomatically altered spessartites from other dikes, except that amphibole, in addition to chlorite, begins to be replaced by magnesite (Fig.3, *d*). In the transition zone, spessartites acquire a light grey colour with a greenish tint. In this zone, amphibole and biotite are no longer preserved, chlorite disappears, plagioclase is completely albitized, and the magnesite content increases. A characteristic feature of the rocks in the transition metasomatic zone is an increase in sericite proportion in mineral composition (Fig.3, *e*). Part of sericite is represented by bright green fuchsite, which causes the greenish tint of the rock. In the transition metasomatic zone relative to the outer zone, the pyrite content increases from 0.5 to 2 vol.%. Spessartites in the inner metasomatic zone are light grey with a beige tint. The mineral composition of the rocks in the inner metasomatic zone is simplified, chlorite and

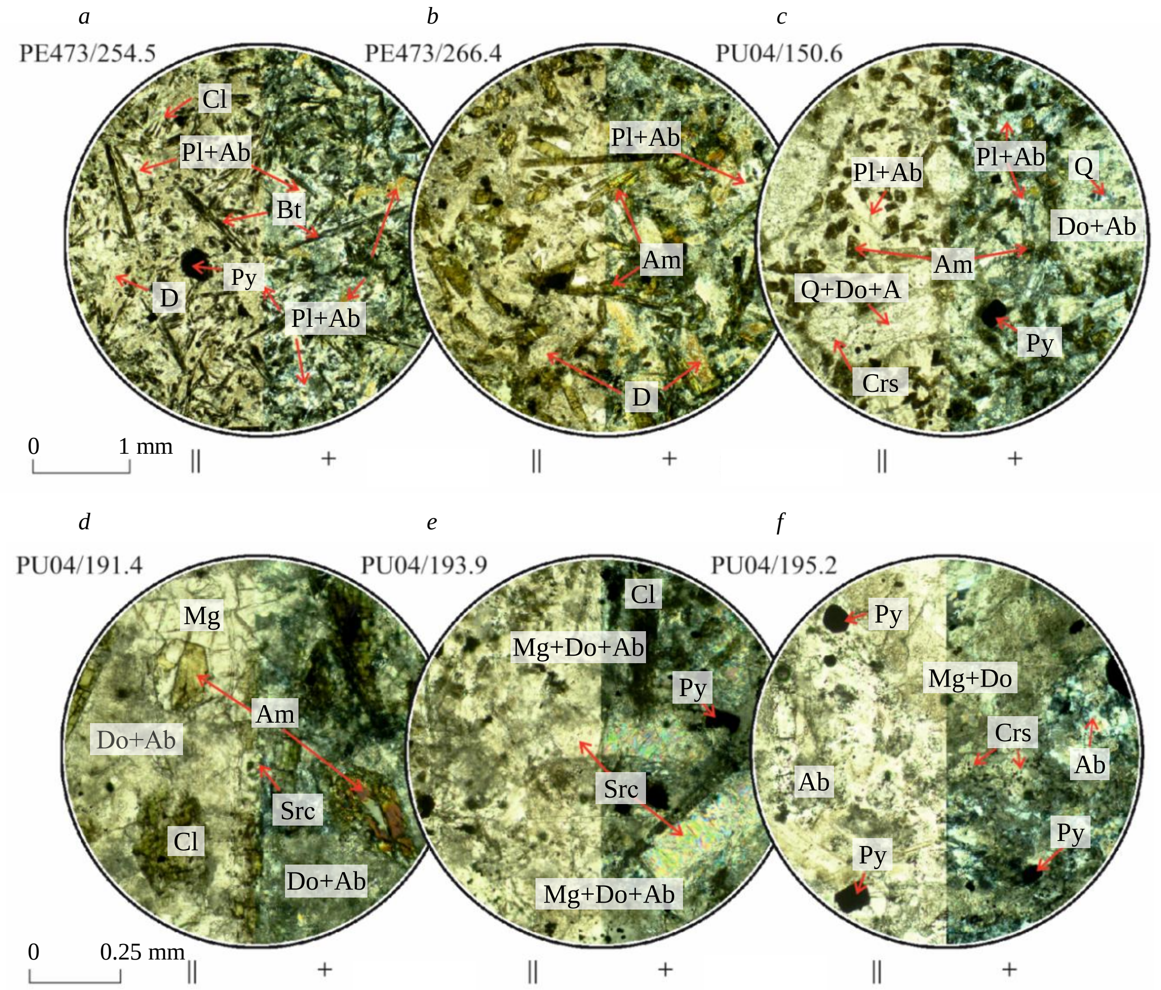

Fig.3. Micrographs of thin sections of kersantite (*a*), spessartite (*b*, *c*)
and metasomatic zones in a dike of altered spessartites: outer (*d*), transition (*e*), and inner (*f*) zone

|| – nicols are parallel, + – nicols are crossed; Ab – albite, Am – amphibole, Bt – biotite, Cl – chlorite,
Crs – chrome spinelide, Do – dolomite, Mg – magnesite, Pl – plagioclase, Py – pyrite, Q – quartz, Src – sericite

sericite almost disappear (Fig.3, *f*). Albite content in the rocks in this zone exceeds 50 vol.%. In addition to albite, developing after plagioclase, independent grains appear – aggregates of this mineral. Pyrite content in the inner metasomatic zone increases to 5 vol.%. The proportion of quartz in the mineral composition of spessartites during the transition from the outer metasomatic zone to the inner one slightly decreases.

Magmatic mineral paragenesis. Amphibole of spessartites is widespread in the form of grains of prismatic habit, to 2 mm in elongation, pleochroic from pale greenish-yellow to brownish-green. In chemical composition (Table 1) it corresponds to magnesiohastingsite [32]. Biotite is present in spessartites and kersantites, forms tabular grains to 1.5 mm in size along the pinacoid plane with a thickness of no more than 0.1 mm (Fig.4, *a*). In thin section it is pleochroic from greyish-green to dark greenish-brown. Biotite belongs to the annite-phlogopite isomorphic series with an admixture of eastonite-siderophyllite component (see compositions in Table 1). Plagioclase is preserved as relics in the bulk (Fig.4, *b*) and has an andesine composition. Accessory chrome-spinel, which is preserved at all stages of metasomatic alterations, can also be attributed to the minerals of magmatic paragenesis. Chrome-spinel is usually observed inside ocelli in the form of rounded, isometric grains (Fig.4, *d*), as well as octahedrons measuring 0.01-0.05 mm, less often in the bulk in the form of grains with a square cross-section, to 0.2 mm in size (Table 1). According to the classification by end members [33], this mineral from spessartites corresponds to aluminous magnesiochromite. Another ubiquitous accessory mineral, which is present in all studied lamprophyre samples, is apatite. Apatite consists of grains elongated in one direction, to 0.1 mm long and 0.01-0.02 mm wide (Fig.4, *c*). In chemical composition it corresponds to fluorapatite [34], has increased SiO_2 and SO_3 contents, low P_2O_5 contents, and reduced sum values. Low sum values may indicate enrichment of apatite in hydroxyl group and carbon, but the used electron microscopy method only enables to assume such a conclusion. Apatite composition changes insignificantly depending on the location in a particular zone of metasomatic alteration of spessartites. From the outer metasomatic zone to the inner one, CaO, P_2O_5 contents and the sum values statistically increase in apatite, which may indicate a decrease in CO_2 and OH proportion in it. A mineral containing Sr, Ba and S, probably a sulphate of the barite-celestine series, is present in apatite in the form of small inclusions.

Table 1

Representative chemical compositions of minerals of metasomatically altered spessartites, wt.%

Sample	PU04/ 191.4	PU04/ 191.4	PU04/ 191.4	PU04/ 191.4	PU04/ 191.4	PU04/ 191.4	PU04/ 191.4	PU04/ 195.2	PU04/ 191.4	PU04/ 191.4	PU04/ 191.4	PU04/ 195.2
Mineral	Am	Am	Bt	Bt	Cl	Cl	Crs	Crs	An	Ab	Ap	Ap
SiO_2	41.04	40.23	37.14	37.81	33.93	34.55	0.83	0.42	53.53	67.62	1.74	1.53
TiO_2	1.48	1.86	0.93	0.92	–	–	0.3	0.43	–	–	–	–
Al_2O_3	14.14	14.30	16.70	16.98	15.86	14.95	18.94	20.32	29.74	20.31	0.27	0.19
Cr_2O_3	–	–	–	–	–	–	47.82	44.02	–	–	–	–
FeO*	11.28	11.87	12.89	12.14	15.61	14.38	17.64	21.67	0.56	–	0.66	0.35
MnO	0.23	0.16	–	0.16	–	–	–	–	–	–	–	–
MgO	13.82	13.53	18.41	18.40	21.52	23.71	13.41	12.98	–	–	0.50	0.43
CaO	11.82	11.90	0.18	0.18	0.11	0.35	–	–	10.41	0.08	52.11	55.28
Na_2O	2.43	2.47	0.65	0.90	–	–	–	–	5.34	11.99	0.73	0.46
K_2O	1.04	1.02	7.66	8.00	–	–	–	–	0.42	–	–	–
P_2O_5	–	–	–	–	–	–	–	–	–	–	34.79	37.14
SO_3	–	–	–	–	–	–	–	–	–	–	2.16	1.57
SrO	–	–	–	–	–	–	–	–	–	–	1.01	0.98
F	–	–	–	–	–	–	–	–	–	–	2.16	2.1
Cl	–	–	–	–	–	–	–	–	–	–	0.44	0.47
O = F, Cl*	–	–	–	–	–	–	–	–	–	–	1.01	0.99
H_2O*	2.05	2.04	4.06	4.11	12.09	12.27	–	–	–	–	–	–
Total	99.33	99.38	98.62	99.60	99.12	100.2	98.94	99.84	100*	100*	95.56	99.51

Estimated formula units

	24 O atoms		22 cations		10 cations		4 O atoms		5 cations and 8 anions		17 cations and 26 anions	
Si	6.04	5.94	2.74	2.76	3.37	3.38	0.03	0.01	2.41	2.94	0.31	0.26
Ti	0.16	0.21	0.05	0.05	0.00	0.00	0.01	0.01	–	–	–	–
Al^{IV}	1.96	2.06	1.26	1.24	0.63	0.62	–	–	–	–	–	–
Al^{VI}	0.49	0.43	0.19	0.22	1.22	1.10	–	–	–	–	–	–
Al	–	–	–	–	–	–	0.70	0.74	1.41	1.04	0.06	0.04
Cr	–	–	–	–	–	–	1.18	1.08	–	–	–	–
Fe^{2+}	1.05	1.12	0.80	0.74	1.29	1.18	0.41	0.42	0.02	–	0.10	0.05
Fe^{3+}	0.34	0.35	0.00	0.00	0.00	0.00	0.05	0.14	–	–	–	–
Mn	0.03	0.02	0.00	0.01	0.00	0.00	–	–	–	–	–	–
Mg	3.03	2.98	2.02	2.00	3.18	3.45	0.63	0.60	–	–	0.13	0.11
Ca	1.86	1.88	0.01	0.01	0.01	0.04	–	–	0.31	0.00	9.78	9.99
Na	0.69	0.71	0.09	0.13	0.00	0.00	–	–	0.61	1.01	0.25	0.15
K	0.20	0.19	0.72	0.74	0.00	0.00	–	–	0.04	–	–	–
P	–	–	–	–	–	–	–	–	–	–	5.16	5.30
S	–	–	–	–	–	–	–	–	–	–	0.28	0.20
Sr	–	–	–	–	–	–	–	–	–	–	0.10	0.10
F	–	–	–	–	–	–	–	–	–	–	1.20	1.12
Cl	–	–	–	–	–	–	–	–	–	–	0.13	0.13

Note. FeO* – total iron FeO and Fe_2O_3. O = F, Cl*, H_2O* – estimated values. 100* – contents are normalized to 100 %. The estimation of formula units was performed by the MineralCalc software with the determination of the Fe^{2+} and Fe^{3+} indices using the G.T.R. Droop method [35].

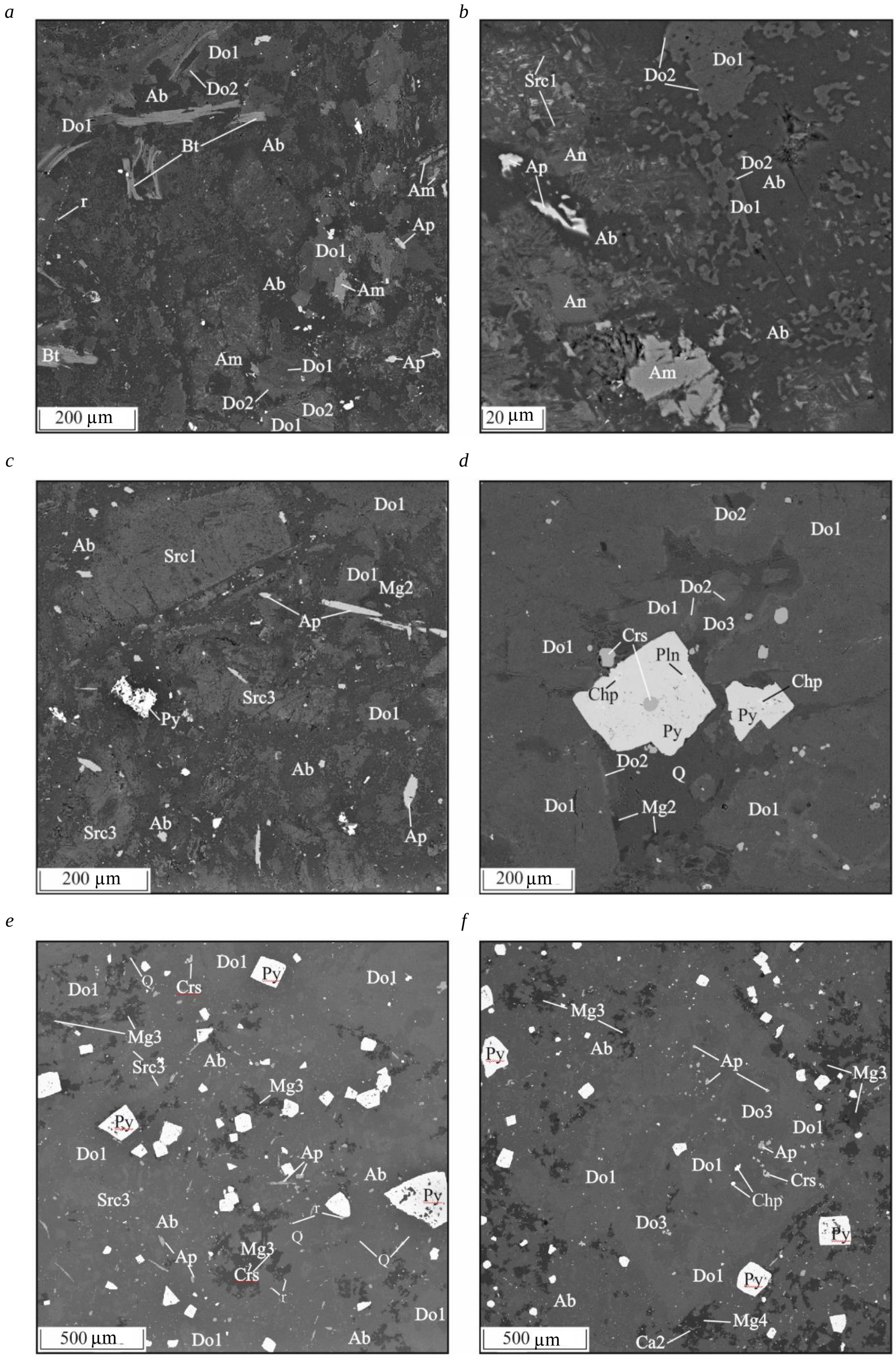

Fig.4. Backscattered electron micrographs of metasomatically altered spessartites.
Outer metasomatic zone, sample PU04/191.4 (*a*, *b*); transition metasomatic zone, sample PU04/193.9 (*c*, *d*);
inner metasomatic zone, PU04/195.2 (*e*, *f*)

An – anorthite, Ap – apatite, Ca – calcite, Chp – chalcopyrite, Pln – pentlandite. For other symbols, see Fig.3

Metasomatic mineral parageneses. Chlorite in lamprophyres of the Peshchernoe deposit replaces amphibole and biotite and corresponds to clinochlore in chemical composition (Table 1). Replacement of amphibole and biotite by chlorite is accompanied by the formation of fine dissemination of rutile with individual grains less than 0.01 mm in size. The main metasomatic mineral in altered spessartites is albite, which makes up about 40 vol.% in the rocks and is a primary plagioclase replacement product. It is found both in independent segregations and in intergrowths with sericite and plagioclase relics with individual grains measuring 0.01-0.02 mm. In metasomatites after spessartites with pronounced metasomatic zoning, albite content in the transition zone increases to 50 vol.% and in the inner zone to 55 vol.%. In the transition and inner metasomatic zones, newly formed albite appears. Unlike the similar mineral replacing andesine, it has independent larger grains to 0.1 mm in size. Carbonate in altered lamprophyres is represented by ferruginous dolomite (Table 2) and makes up 35-40 vol.% in the rocks. Zoning is observed in dolomite grains, in which the central part of the dolomite grains is less ferruginous than the marginal part (Fig.4, *b*, *d*, *f*).

Table 2

Chemical composition of carbonates, wt.%

N	Sample	Mineral	$FeCO_3$	$MnCO_3$	$MgCO_3$	$CaCO_3$	$SrCO_3$	Total
1	PE472/264.8	Do1	10.43	1.18	30.64	57.75	0.00	100.0
2	PU04/191.4	Do1	9.20	0.82	30.81	59.17	0.00	100.0
3	PU04/191.4	Do1	10.98	0.87	30.48	57.67	0.00	100.0
4	PU04/191.4	Do1 c	8.83	1.71	31.26	58.20	0.00	100.0
5	PU04/191.4	Do2 e	17.99	0.67	27.20	53.01	1.12	100.0
6	PU04/193.9	Do1	9.90	0.52	30.56	59.02	0.00	100.0
7	PU04/193.9	Do1	10.16	0.66	29.24	59.95	0.00	100.0
8	PU04/193.9	Do1 c	9.61	1.87	31.49	57.03	0.00	100.0
9	PU04/193.9	Do2 e	14.60	2.76	28.19	53.12	1.33	100.0
10	PU04/193.9	Do1 c	11.00	0.51	31.07	57.09	0.32	100.0
11	PU04/193.9	Do2 e	12.49	3.23	29.23	53.84	1.20	100.0
12	PU04/193.9	Do3	5.67	1.02	35.38	56.40	1.53	100.0
13	PU04/195.2	Do1	8.94	1.40	31.11	58.56	0.00	100.0
14	PU04/195.2	Do3 c	3.66	1.31	35.79	57.87	1.37	100.0
15	PU04/195.2	Do1 e	8.49	1.18	32.56	57.77	0.00	100.0
16	PU04/195.2	Do3 c	4.26	1.03	35.77	57.59	1.36	100.0
17	PU04/195.2	Do1 e	10.90	1.79	29.65	57.38	0.29	100.0
18	PU04/191.4	Mg1	59.03	0.98	37.99	2.00	0.00	100.0
19	PU04/191.4	Mg1	56.50	1.30	40.48	1.73	0.00	100.0
20	PU04/193.9	Mg2	36.47	0.55	62.49	0.49	0.00	100.0
21	PU04/193.9	Mg2	33.94	1.94	62.89	1.23	0.00	100.0
22	PU04/195.2	Mg3	13.98	0.47	85.05	0.50	0.00	100.0
23	PU04/195.2	Mg3	13.12	0.00	86.67	0.22	0.00	100.0
24	PU04/195.2	Mg4	8.38	0.00	90.72	0.91	0.00	100.0
25	PU04/195.2	Ca1	1.88	0.00	4.09	94.03	0.00	100.0
26	PU04/195.2	Ca1	1.71	0.00	4.55	93.10	0.63	100.0
27	PU04/195.2	Ca2	1.49	0.39	1.03	97.10	0.00	100.0

Notes: c – grain centre; e – grain edge; 18, 19 – replaces amphibole; 25, 26 – at the boundary between dolomite and magnesite; 27 – fills a fracture in magnesite.

In addition to dolomite chemical composition change within a single grain, variations in composition are observed during the transition from one metasomatic zone to another. Three types of dolomite can be distinguished by chemical composition. In the outer and transition metasomatic zones, the grains centre is represented by dolomite-1 (Do1 in Table 2) with 8.5-11.0 wt.% $FeCO_3$. Dolomite-2 (Do2) from the marginal part of the grains is more ferruginous. In the outer metasomatic zone, $FeCO_3$ content in it reaches 18.0 wt.%, in the transition zone – 12.5-14.6 wt.%. In addition to a higher iron content, Do2 has a $SrCO_3$ content of 1.1-1.3 wt.%, while in Do1 the content of this component is to 0.3 wt.%. In the inner metasomatic zone, the central part of the grains is dolomite-3 (Do3), with a $FeCO_3$ content of 3.7-4.3 wt.% and $SrCO_3$ of about 1.5 wt.%. The marginal part of the dolomite grains in the inner metasomatic zone is similar in chemical composition to Do1. In addition to dolomite, magnesite appears in the outer metasomatic zone. Magnesite replaces porphyritic phenocrysts of amphibole and in chemical composition corresponds to breunnerite (Mg1 in Table 2), with $FeCO_3$ content of 56-59 wt.%. In the transition metasomatic zone, magnesite becomes less ferruginous (Mg2) and has $FeCO_3$ content of 34-36.5 wt.%. In the inner metasomatic zone, two types of magnesite (Mg3 and Mg4) are present, differing in iron content. In the first type $FeCO_3$ is from 13 to 14 wt.%, in the second – about 8.4 wt.%.

Thus, in the direction from the outer metasomatic zone to the inner one, the iron content of carbonates in altered spessartites decreases. In the inner metasomatic zone, in addition to dolomite and magnesite, small calcite segregations were found. In one case, calcite is located between dolomite and magnesite (Ca1 in Table 2), in the other it fills a microfracture in magnesite (Ca2, Fig.4, *f*). Sericite in metasomatically altered spessartites belongs to the muscovite – paragonite isomorphic series (Table 3). In different parts of the metasomatic halo, the percentage of sericite varies and its chemical composition changes. In the outer metasomatic zone, sericite makes up 5 vol.%. It is dominated by the paragonite end member with Na_2O and K_2O contents of 5 wt.% each (Src1 in Table 3). In the transition metasomatic zone, the amount of sericite increases to 10 vol.% with the size of individual grains being 0.5-1 mm (Fig.4, *c*).

According to the chemical composition, three types of sericite are distinguished in this zone. The first type is close to sericite from the outer zone with a slight predominance of the paragonite end member and Na_2O and K_2O contents of 3.2 and 7.0 wt.%, respectively. In the second type of sericite (Src2), the muscovite end member predominates, and to 10 mol.% of the fuchsite end member is observed. The contents in it are, wt.%: Na_2O 1.6-1.8, K_2O 5.5-5.7, and Cr_2O_3 to 1.6. Sericite of the third type is muscovite (Src3) with Na_2O content of about 0.6 wt.% and K_2O 9.4 wt.%. In the inner metasomatic zone, sericite content is 1-2 vol.% and it is represented by muscovite.

Table 3

Chemical composition of sericite, wt.%

Component	PU04/191.4	PU04/193.9	PU04/193.9	PU04/193.9	PU04/193.9	PU04/195.2	PU04/195.2	PU04/195.2
	Src1	Src1	Src2	Src2	Src3	Src3	Src3	Src3
SiO_2	54.66	52.49	49.80	49.69	48.63	48.98	49.38	49.65
Al_2O_3	28.62	30.14	35.25	35.34	32.64	32.05	32.98	31.15
Cr_2O_3	–	–	1.59	1.46	–	–	–	–
FeO*	1.13	1.39	0.30	0.45	2.5	2.48	1.85	2.98
MgO	0.36	1.25	0.82	0.83	1.74	2.29	1.98	1.81
CaO	0.92	–	0.30	0.28	–	–	–	–
Na_2O	4.72	3.16	1.60	1.83	0.58	0.45	0.31	0.28
K_2O	4.95	6.96	5.68	5.48	9.39	9.22	8.94	9.60
H_2O*	4.64	4.60	4.60	4.61	4.53	4.54	4.57	4.52
Total	100.0	100.0	100.0	100.0	100.0	100.0	100.0	100.0
Content of end-members, mol.%								
Muscovite	33	44	52	49	74	73	79	77
Paragonite	62	46	34	38	11	10	7	6
Celadonite	5	10	5	5	15	17	14	17
Fuchsite	–	–	9	8	–	–	–	–

Note. Muscovite $KAl_2(AlSi_3O_{10})(OH_2)$, paragonite $NaAl_2(AlSi_3O_{10})(OH_2)$, celadonite $K(Mg,Fe^{3+})(Si_4O_{10})(OH_2)$, fuchsite $K(Al,Cr)_3(Si_3O_{10})(OH_2)$ were used as end members.

Sulphides. In the metasomatically altered lamprophyres of the Peshchernoe deposit, sulphides are mainly represented by pyrite, the content of which averages 0.5 vol.%. Pyrite has sections of predominantly complex shape, less often rectangular, with an average size of 0.01 mm, rarely to 0.05 mm. In different metasomatic zones developed along the spessartite dike, the amount and morphology of pyrite vary. In the outer metasomatic zone, the content and character of pyrite are similar to those observed in the other lamprophyre dikes. In the transition metasomatic zone, pyrite increases to 2 vol.%, the sections also have a predominantly complex shape with the presence of rectangles, the size of the sections is on average 0.01-0.03 mm, rarely to 0.2 mm. In the inner metasomatic zone, pyrite increases to 5 vol.%, the average grain size increases to 0.05 mm. The shape of the pyrite sections in the inner zone is mainly rectangular, sections corresponding to the shape of grains in the form of pyritohedra appear (Fig.4, *e*). The chemical composition of pyrite is quite consistent, with small variations in the content of Co and Ni impurities. An As impurity was found in a single grain from the inner metasomatic zone. Sphalerite, chalcopyrite, and pentlandite are present in the form of inclusions in pyrite, as well as small independent grains (Fig.4, *d*, *f*).

Petrochemical characteristics of rocks. The contents of petrogenic components and rare elements in lamprophyres of the Peshchernoe gold deposit are given in Table 4. Low SiO_2 contents and high loss on ignition (LOI) values in lamprophyres indicate metasomatic alterations and can serve as a criterion for assessing their manifestation scale. In the least altered spessartites, the SiO_2 contents are 40-41 wt.% with a LOI of 12.5-13.5. In the most altered samples, these values are 34.7-36 wt.% and 15.5-17.1 wt.%, respectively. In kersantites from the Peshchernoe deposit, the SiO_2 values are higher than in spessartites, from 42 to 45 wt.%, and the LOI is lower – 8-10 wt.%.

Table 4

Content of petrogenic components (wt.%), gold (mg/t), and rare elements (g/t) in lamprophyres from the Peshchernoe gold deposit

Component	Sample											
	PU03/96.6	PU04 150.6	PU04/167.9	PE472/264.8	PU04/191.4	PU04/193.9	PU04/195.2	PU04/198.6	PE472/179.5	PE473/254.5	Spec_B	Kers_B
	1	2	3	4	5	6	7	8	9	10	11	12
SiO_2	34.72	40.66	36.03	39.82	38.52	35.65	38.89	40.89	44.81	42.39	46.04	52.55
TiO_2	0.64	0.83	0.55	0.73	0.67	0.78	0.71	0.78	1.22	1.18	0.72	1.19
Al_2O_3	11.85	12.79	10.27	11.81	10.45	12.02	11.18	11.58	14.62	14.18	12.54	12.08
FeO*	5.17	7.54	6.20	7.53	7.76	6.39	5.27	7.54	7.34	7.24	9.82	5.90
MnO	0.12	0.13	0.13	0.16	0.14	0.13	0.11	0.13	0.19	0.14	0.16	0.12
MgO	8.12	9.62	12.23	13.44	12.44	10.22	11.28	10.46	9.59	8.04	13.02	8.34
CaO	15.38	10.60	11.68	10.12	10.75	10.29	9.89	11.43	8.03	9.48	8.17	6.7
Na_2O	4.67	3.04	3.92	2.72	2.75	4.24	5.01	3.07	3.19	4.98	2.1	2.4
K_2O	0.15	0.58	0.42	0.18	0.40	0.77	0.21	0.56	1.32	0.24	0.66	5.0
P_2O_5	0.15	0.40	0.21	0.30	0.29	0.31	0.27	0.34	0.71	0.72	0.15	0.84
LOI	15.42	13.05	16.06	12.44	15.02	17.11	13.37	12.57	7.96	10.21	5.8	4.3
S	3.15	0.33	1.94	0.30	0.28	1.73	3.24	0.21	0.44	0.64	0.22	0.16
Total	99.56	99.57	99.64	99.54	99.47	99.63	99.44	99.56	99.41	99.43	99.75	99.78
Au	–	–	–	<0.8	2.8	4.3	23.0	8.2	–	–	–	–
Li	0.86	25.1	11.4	22.5	22.2	2.77	7.82	17.6	6.53	14.6	–	–
Be	0.46	0.89	0.59	0.80	0.74	0.81	0.44	0.91	1.18	1.19	–	–
Sc	20.6	24.2	26.9	26.8	28.0	25.4	26.2	25.8	20.2	20.4	–	–
V	129	183	128	164	148	168	116	170	212	219	–	–
Cr	178	333	480	535	501	454	273	348	307	292	–	–
Co	30.6	34.1	38.6	39.3	41.4	36.2	39.6	36.4	28.3	29.7	–	–
Ni	175	185	265	254	253	215	254	232	136	131	–	–
Cu	40.9	54.7	49.1	49.3	35.6	53.8	55.4	50.1	85.2	80.6	–	–
Zn	45.6	56.8	47.3	58.5	50.1	51.2	46.0	58.0	64.8	69.9	–	–
Ga	11.6	13.0	10.0	11.7	11.0	11.0	10.8	12.4	14.8	15.2	–	–
As	212	9.07	110	3.80	2.93	63.7	191.1	2.55	9.32	6.67	–	–
Rb	2.51	9.15	6.16	1.91	6.52	10.7	3.08	6.46	6.37	19.8	–	–

End of Table 4

Component	Sample											
	PU03/ 96.6	PU04 150.6	PU04/ 167.9	PE472/ 264.8	PU04/ 191.4	PU04/ 193.9	PU04/ 195.2	PU04/ 198.6	PE472/ 179.5	PE473/ 254.5	Spec_B	Kers_B
	1	2	3	4	5	6	7	8	9	10	11	12
Sr	1618	1060	851	665	969	732	820	1236	1091	702	–	–
Y	10.5	14.5	10.6	14.1	12.9	13.4	13.4	14.9	17.8	18.0	–	–
Zr	66.7	91.8	72.4	91.2	90.2	75.3	74.6	93.7	134	132	–	–
Nb	1.74	2.87	1.43	1.30	1.57	1.10	0.85	2.48	4.41	7.58	–	–
Mo	0.70	0.18	0.54	0.13	0.10	<0.10	<0.10	0.42	1.18	1.00	–	–
Cd	0.24	0.25	0.16	0.15	0.16	0.17	0.15	0.15	0.19	0.17	–	–
Sn	0.31	0.55	0.39	0.64	0.44	0.45	0.31	0.53	0.87	0.80	–	–
Sb	2.78	2.64	1.19	0.43	0.38	0.87	8.46	1.14	0.36	0.84	–	–
Cs	0.07	0.84	0.41	0.65	0.88	0.63	0.29	0.53	0.68	0.61	–	–
Ba	351	829	321	872	472	244	531	954	368	678	–	–
La	34.0	47.8	35.3	42.1	39.8	34.6	36.4	45.7	54.7	43.5	32.6	–
Ce	67.4	101	68.3	86.3	83.6	69.8	70.7	93.8	110	93.2	69.8	–
Pr	8.61	12.5	8.48	11.2	10.3	8.87	9.09	11.9	13.5	11.0	9.22	–
Nd	35.6	49.0	34.4	43.8	40.4	36.9	38.7	46.0	50.9	41.7	36.3	–
Sm	6.17	8.15	5.92	7.39	6.89	6.51	6.74	7.69	7.87	6.98	6.08	–
Eu	1.68	2.34	1.63	2.18	1.93	1.70	1.88	2.28	2.21	2.31	1.85	–
Gd	5.03	6.69	4.94	6.20	5.62	5.34	5.48	6.43	6.85	6.12	4.41	–
Tb	0.54	0.71	0.52	0.66	0.60	0.60	0.59	0.69	0.75	0.73	0.48	–
Dy	2.48	3.23	2.40	3.00	2.82	2.75	2.74	3.20	3.53	3.65	2.74	–
Ho	0.42	0.54	0.43	0.54	0.49	0.47	0.46	0.56	0.64	0.66	0.51	–
Er	1.23	1.55	1.20	1.49	1.42	1.38	1.36	1.58	1.81	1.82	1.43	–
Tm	0.14	0.18	0.16	0.18	0.17	0.15	0.15	0.19	0.22	0.23	0.20	–
Yb	0.99	1.19	0.97	1.16	1.11	1.05	1.07	1.25	1.48	1.50	1.36	–
Lu	0.14	0.17	0.13	0.18	0.16	0.17	0.15	0.18	0.22	0.20	0.21	–
Hf	1.80	2.21	1.68	2.15	2.24	1.80	1.85	2.26	3.07	2.96	–	–
Ta	2.65	0.64	0.37	0.33	0.34	0.31	0.34	0.40	0.39	0.53	–	–
W	0.82	0.14	0.09	<0.08	<0.08	0.16	0.21	<0.08	0.22	0.32	–	–
Pb	9.04	7.51	4.39	4.93	2.67	3.39	4.16	6.69	5.10	5.82	–	–
Th	5.00	6.54	5.00	5.69	5.60	5.16	4.97	6.43	5.53	5.55	–	–
U	1.10	1.49	1.17	1.34	1.29	1.15	1.10	1.45	1.28	1.30	–	–

Notes: 1-4 – spessartite dikes; 5-8 – samples from one spessartite dike: 5 – marginal part, hanging wall, outer metasomatic zone, 6 – transition metasomatic zone, 7 – central part, inner metasomatic zone, 8 – marginal part, footwall, outer metasomatic zone; 9, 10 – kersantite dikes; 11, 12 – rocks of the Vorontsovskoe gold ore deposit according to [25, 36]: 11 – spessartite (petrogenic elements – sample N 933, REE – sample N 34-2/17), 12 – kersantite. FeO* – total iron FeO and Fe_2O_3.

Another pair of components that correlates with the degree of metasomatic alteration of lamprophyres are Na_2O and S. In less altered rocks, the Na_2O content is 2.7-3.1 wt.%, and S is about 0.3 wt.%, in more altered samples 4.7-5 wt.% and 3.2 wt.%, respectively. The two pairs of petrogenic components listed above do not always correlate with each other. For example, spessartites from the inner metasomatic zone, which actually underwent the greatest metasomatic processing, have high Na_2O and S contents with average SiO_2 and LOI values.

TiO_2 content in lamprophyres varies depending on the rock type, amounting to 1.2 wt.% in kersantites and 0.5-0.8 wt.% in spessartites. In addition, kersantites have higher Al_2O_3 contents compared to spessartites. Widely varying K_2O contents in kersantites from 0.2 to 1.3 wt.% indicate the replacement of biotite by secondary minerals during metasomatism with the removal of potassium from the rock, which is confirmed by petrographic observations. In altered spessartites, K_2O is 0.2-0.8 wt.%. MnO, FeO, MgO, and CaO contents in kersantites and less altered spessartites of the Peshchernoe deposit have similar values. Variations in the total FeO content in spessartites correlate with the degree of metasomatic alteration. In the least altered spessartites, FeO is 7.5 wt.%, decreasing with increasing metasomatic alteration to 5.2 wt.%.

Thermal analysis was performed for samples from a spessartite dike with evident metasomatic zoning. It allows estimating the contents of OH and CO_2 components in these rocks. Mass losses during decomposition of dolomite and magnesite were 12-17 %, which leads to the conclusion that the CO_2 content in the rocks is 12-17 wt.%. The OH contents were estimated from the mass change during chlorite decomposition and amounted to 1.3 wt.%. Part of the mass decrease during thermal analysis is due to adsorption moisture in the preparation and pyrite decomposition. The total mass changes in the studied samples were 14.2-18 wt.%, which is quite close to the obtained values of loss on ignition measured as part of the X-ray fluorescence analysis.

Geochemical characteristics of rocks. Spessartites and kersantites of the Peshchernoe gold deposit differ in the content of individual rare elements (Table 4, Fig.5 and 6). Kersantites have higher values of Be, V, Cu, Zn, Y, HREE, Zr, Hf, Nb, Mo, Sn, W relative to spessartites, while the latter have higher Cr, Co, and Ni contents. Variations in the rare element contents are observed in spessartites depending on the degree of metasomatic alteration of rocks. More altered spessartites have lower Li, Zr, Hf, and REE contents and higher As, Sb, and W contents. The above-mentioned geochemical features of lamprophyres are reflected in Fig.5 and 6, where the absolute contents of the element in the rock are normalized to chondrite C1 [37] and the average content in calc-alkaline lamprophyres according to [18], respectively. Spessartites in these diagrams are divided into three groups: weakly, moderately, and strongly metasomatically altered. Distribution of samples by the degree of metasomatic alteration was made according to petrographic, petrochemical, and geochemical data. Au contents were measured in one of the dikes of less altered spessartites, as well as in metasomatites after a dike of spessartites with pronounced metasomatic zoning. In weakly altered spessartites, Au content was below the detection limit. The rocks of the inner metasomatic zone contain, mg/t: 23 gold, in the transition zone 4, in the outer zone in the hanging wall of the dike 3, in the outer zone in the footwall 8. Note that the metasomatites of the outer zone in the footwall of the dike have higher Sb, Zn, Pb, Ba, Mo, Th, and U contents than in the hanging wall.

Discussion of the results

According to petrographic and petrochemical observations, lamprophyres of the Peshchernoe deposit correspond to spessartites and kersantites that underwent significant metasomatic alterations. In addition to lamprophyre dikes, the deposit also contains andesitic dikes. A similar compositionally diverse dike complex was described at the Vorontsovskoe gold deposit [25, 36], located approximately 8 km southeast of the Peshchernoe deposit. The observed spatial relationship between gold mineralization and dike series, including spessartites, kersantites, and andesitic rocks, can serve as a prospecting criterion for this region.

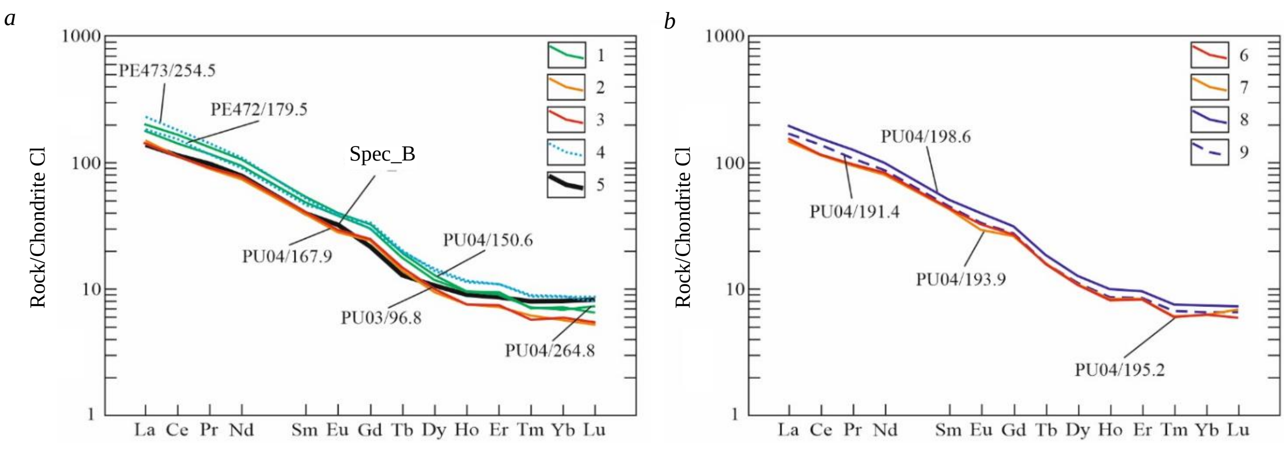

Fig.5. Rare earth element contents in lamprophyres of the Peshchernoe deposit, normalized to chondrite C1 [37]:

a – individual dikes of spessartites and kersantites (1-3 – spessartites of the Peshchernoe deposit: 1 – weakly metasomatically altered, 2 – moderately altered, 3 – strongly altered; 4 – kersantites of the Peshchernoe deposit; 5 – spessartites of the Vorontsovskoe deposit according to [36]);
b – metasomatic zones in the dike of altered spessartites (6 – central part of the dike, inner metasomatic zone; 7 – transitional metasomatic zone; 8 – marginal part of the dike, footwall, outer metasomatic zone; 9 – marginal part of the dike, hanging wall, outer metasomatic zone)

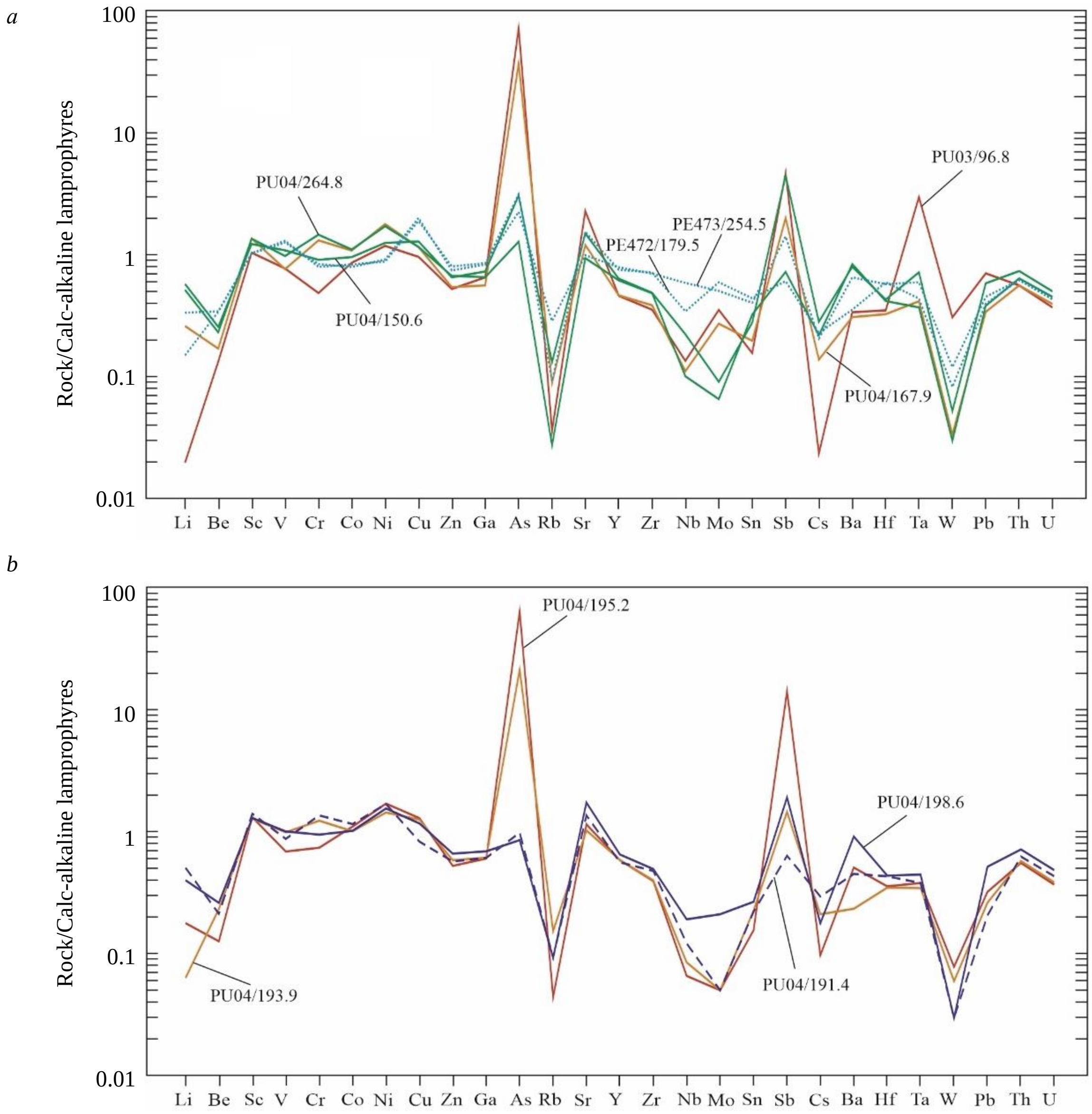

Fig.6. Rare element contents in lamprophyres of the Peshchernoe deposit,
normalized to the average content in calc-alkaline lamprophyres according to [18]:
a – individual spessartite and kersantite dikes; *b* – metasomatic zones in a dike of altered spessartites
See Fig.5 for legend

The measured attitude of the lamprophyre dike coincides with the direction and dip angle of the ore-controlling faults. The presence of discontinuous faults, which are fluid conductors and usually filled with lamprophyre dikes, is noted at many gold deposits [11, 17]. Dikes of lamprophyres and andesitic rocks are pre-ore, as evidenced by the superimposed metasomatic mineral associations. Metasomatic alterations at the Peshchernoe deposit are controlled mainly by a series of faults striking northeast, forming a metasomatic halo enveloping the fault zone. Structurally, faults dipping southeast at an angle of about 60°, dike bodies, metasomatic halos and mineralized zones represent one system, and the host volcanogenic-sedimentary rocks gently dipping to the northeast represent another one.

The diagram of the arrangement of additive geochemical halos of Ag + Sb + As [30] to the south of the Peshchernoe deposit reflects a series of linear, near N-S elongated geochemical anomalies, which spatially coincide with the Zapadno-Peshcherninskii fault. It can be assumed that the geochemical halos record the influence of fluids entering through fault systems. In the deposit area, elongation of the geochemical halos takes on a northeastern direction and coincides with the orientation of the faults in which the mineralized zones are localized. The northeast striking fault zone occurs subconformably with the contact of the volcanogenic-sedimentary rocks of the Turinskaya Fm. and the coeval basalt strata. Probably, basalts served as a screening structure for hydrothermal solutions.

The data on the structural position of mineralized ore zones, faults, dike bodies, metasomatic halos, and host volcanogenic-sedimentary rocks suggest that the alteration system of the Peshchernoe deposit is tectonogenic. Probably, dikes of rocks of andesitic composition, lamprophyres were intruded along the northeast striking fault zone at different geological times, and subsequently it became a channel for hydrothermal fluids, including ore-bearing ones. The influence of primary orientation of volcanogenic-sedimentary rocks for gold, as was proposed for Vorontsovskoe [24], seems unlikely in the Peshchernoe deposit area.

To assess the influence of metasomatism on the chemical composition of lamprophyres, it is necessary to determine the primary rock composition. It was not possible to detect unaltered lamprophyres in the Peshchernoe deposit drillhole core. The average composition of lamprophyres from the Vorontsovskoe ore field [25, 36] and calc-alkaline lamprophyres according to [18] are quite close, which may indicate an insignificant degree of their alteration by metasomatism. Therefore, we accepted the compositions of spessartites and kersantites from the Vorontsovskoe deposit [25, 36] as a possible educt. Individual compositions of these rocks are given in Table 4.

The least altered spessartites and kersantites from the Peshchernoe deposit differ from similar rocks of the Vorontsovskoe deposit by a lower SiO_2 content and higher CaO, Na_2O, and LOI values. In addition, spessartites from Peshchernoe have a lower total FeO content, compared with spessartites from the Vorontsovskoe deposit. Kersantites from Peshchernoe contain less K_2O, relative to kersantites from the Vorontsovskoe deposit. The REE contents in spessartites from the Peshchernoe and Vorontsovskoe deposits are almost identical (see Fig.5). The differences in the contents of petrogenic components in lamprophyres from the Peshchernoe and Vorontsovskoe deposits are the result of a higher degree of metasomatic alterations in the former. Accordingly, the initial metasomatic stage observed in lamprophyres from the Peshchernoe deposit was accompanied by SiO_2, FeO, K_2O removal from the rocks and CaO, Na_2O, CO_2 supply. REE contents remained without significant changes.

A more detailed analysis can be made of the substance balance during the next stage of metasomatism, expressed in the development of metasomatic mineral parageneses that form individual metasomatic zones in one of the dikes of altered spessartites. The alterations that occurred when metasomatites formed at this stage led to a change in the rock density. Spessartites of the outer metasomatic zone (sample PU04/191.4) have a density of 2.8 g/cm^3, in the transition zone (sample PU04/193.9) it increases to 2.85 g/cm^3, and in the inner zone (sample PU04/195.2) it is 2.86 g/cm^3. The estimation results are presented in Table 5; N_i^v is the number of element atoms in a geometric volume of rock in 10,000 Å^3: $N_i^v{}_1$ in metasomatically altered spessartites of the outer, $N_i^v{}_2$ in the transition, and $N_i^v{}_3$ in the inner zones; ΔN_i^v is the difference between the number of element atoms in a geometric volume of rock in 10,000 Å^3 of the source and resulting rock: $\Delta N_i^v{}_{1\text{-}2}$ in the outer and transition, $\Delta N_i^v{}_{2\text{-}3}$ in the transition and inner, $\Delta N_i^v{}_{1\text{-}3}$ in the outer and inner zones; ΔN_i^v is designated with a plus if the element is supplied and with a minus if it is removed; $\Delta N_i^v/N_i^v{}_1$ is the relative change in the number of element atoms as a percentage of the number of element atoms in the source rock, in our case, the number of element atoms in metasomatically altered spessartites of the outer zone. Figure **7** shows the relative changes in the number of element atoms when passing from the outer metasomatic zone to the transition zone and from the transition zone to the inner one, the line is the result of these changes, corresponding to the difference in the number of element atoms between the outer and inner metasomatic zones.

Table 5

Estimation of the substance balance during the alteration of spessartites at the sodic stage of metasomatism

Elements	Number of atoms per 10,000 Å^3			Supply-removal per 10,000 Å^3					
	PU04/191.4	PU04/193.9	PU04/195.2	Absolute differences			Relative to $N_i^v{}_1$, %		
	$N_i^v{}_1$	$N_i^v{}_2$	$N_i^v{}_3$	$\Delta N_i^v{}_{1\text{-}2}$	$\Delta N_i^v{}_{2\text{-}3}$	$\Delta N_i^v{}_{1\text{-}3}$	$\Delta N_i^v{}_{1\text{-}2}/N_i^v{}_1$	$\Delta N_i^v{}_{2\text{-}3}/N_i^v{}_1$	$\Delta N_i^v{}_{1\text{-}3}/N_i^v{}_1$
Si	110	103	112	–7	+9	+2	–6.36	+8.18	+1.82
Ti	1.43	1.70	1.57	+0.27	–0.13	+0.14	+18.88	–9.09	+9.79
Al	35.0	40.9	38.5	+5.9	–2.4	+3.5	+16.86	–6.86	+10.00
Fe^{2+}	18.5	15.5	12.9	–3.0	–2.6	–5.6	–16.22	–14.05	–30.27
Mn	0.33	0.31	0.27	–0.02	–0.04	–0.06	–6.06	–12.12	–18.18
Mg	52.7	44.0	49.1	–8.7	+5.1	–3.6	–16.51	+9.68	–6.83
Ca	32.8	31.9	30.9	–0.9	–1.0	–1.9	–2.74	–3.05	–5.79
Na	15.2	23.8	28.3	+8.6	+4.5	+13.1	+56.58	+29.61	+86.18
K	1.47	2.84	0.77	+1.37	–2.07	–0.70	+93.20	–140.82	–47.62
P	0.69	0.75	0.68	+0.06	–0.07	–0.01	+8.70	–10.14	–1.45
S	1.47	9.37	17.72	+7.90	+8.35	+16.25	+537.41	+568.03	+1105.44
CO_2	56.7	64.3	48.2	+7.6	–16.1	–8.5	+13.40	–28.40	–14.99
OH	12.4	–	–	–12.4	–	–12.4	–100.00	–	–100.00
O	526	502	481	–24	–21	–45	–4.56	–3.99	–8.56
Total +	–	–	–	+31.7	+26.95	+34.99	+3.67	+3.12	+4.05
Total –	–	–	–	–56.02	–45.41	–77.77	–6.48	–5.25	–8.99
Total	864.69	840.37	821.91	–24.32	–18.46	–42.78	–2.81	–2.13	–4.94

Note. The estimation was performed using the atomic volume conversion by Yu.V.Kazitsyn and V.A.Rudnik [38].

Four groups of elements can be distinguished after a matter analysis. The first group is represented by S and Na, which are supplied into the rocks of the transition and inner metasomatic zones. The second group consists of relatively inert elements at this stage of metasomatism: Al, Ti, Si, P, Ca, Mg. Elements of the third group are removed from the rocks. They include Mn, Fe, and OH. The fourth group of elements is represented by K and CO_2. The amounts of these components increase in the transition zone and decrease significantly in the inner one. We have concluded that this is the result of K and CO_2 redistribution from the inner metasomatic zone to the rocks of the transition zone, and not their removal by metasomatizing solutions. Negative values of the resulting relative changes in K and CO_2 contents can be due to the fact that the transition metasomatic zone is twice thick as the inner one.

The supply and removal of rare elements at the sodic stage of metasomatism is illustrated in Fig.5, *b*. The rocks in the inner metasomatic zone have higher Au, As, Sb, and W contents relative to spessartites in the outer zone, which indicates the supply of these elements as a result of metasomatism, while Li is removed from the rocks. Spessartites with a moderate and strong degree of metasomatic alterations demonstrate a slight depletion in REE relative to less altered rocks with the preservation of the REE spectra shape (see Fig.5). The studied spessartite dike is outside the ore zone (see Fig.2, *b*). However, the distribution of elements observed in it may reflect general patterns. The rocks in the dike footwall have higher Au, Sb, Zn, Pb, Ba, Mo, Th, and U contents compared to the rocks in the hanging wall. This is consistent with the position of ore zones in the footwall of ore-controlling faults and the absence of mineralization in metasomatically altered rocks of the hanging wall.

Two stages of metasomatism can be distinguished in metasomatic alterations observed in the Peshchernoe deposit spessartites: carbon dioxide and subsequent sodic. During carbon dioxide metasomatism, dark-coloured minerals are replaced by chlorite, albitization and sericitization of plagioclase occur. Ferruginous dolomite is formed under the influence of a significant supply of CO_2. The forming mineral paragenesis corresponds to the outer metasomatic zone during listvenization of gabbro [20, 39, 40]. Alkaline (sodic) metasomatism is superimposed on the mineral metasomatic

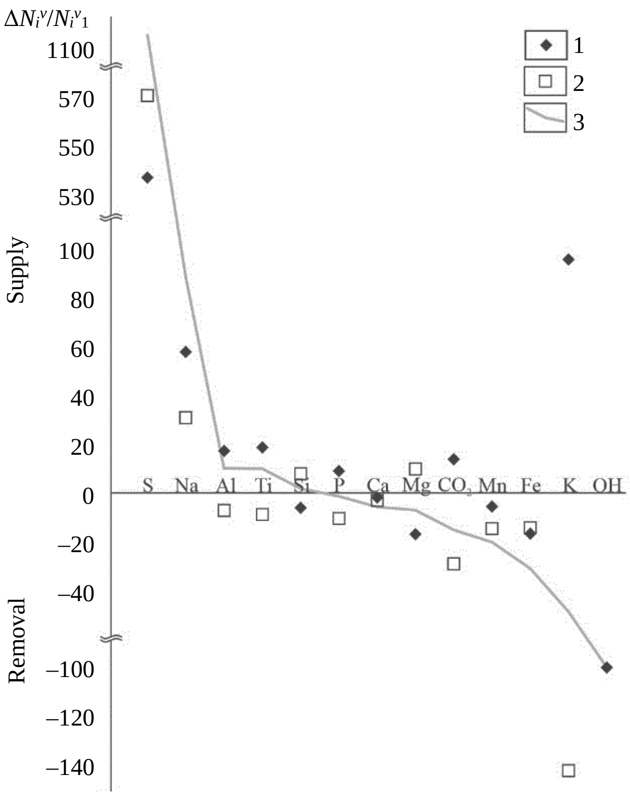

Fig.7. Supply-removal of elements during the sodic stage of metasomatic alteration of spessartites
ΔN_i^v – difference between the number of element atoms in 10,000 Å^3 of the source and resulting rocks; $N_i^v{}_1$ – number of element atoms in 10,000 Å^3 of metasomatically altered spessartites of the outer zone

Alterations during transition:
1 – from the outer metasomatic zone to the transition zone;
2 – from the transition metasomatic zone to the inner one;
3 – the resulting line of alterations corresponding to the difference in the number of element atoms between the outer and inner metasomatic zones

paragenesis of the first stage. Chlorite and relics of magmatic dark-coloured minerals are replaced by magnesite, the supply of Na leads to the appearance of newly formed albite, and as a result of the supply of S, pyrite is formed, which concentrates iron from other minerals. As a result of the sodic stage of metasomatism, the iron content in carbonates decreases in the direction from the outer metasomatic zone to the inner one, whereas the opposite trend was described for listvenization [40]. By high sodium content, formed metasomatites are similar to eisites. They differ from the latter by a significant supply of S and the absence of hematite [41, 42]. The absence of hematization and the binding of iron into pyrite may indicate a higher felsicity of metasomatizing solutions than during the formation of classical eisites [41].

In addition to alterations observed in lamprophyres, propylitized rocks are present in the peripheral areas of the deposit. Propylites and metasomatic alterations of the carbon dioxide stage are widespread in the Peshchernoe deposit area, and the influence of sodic metasomatism has a more local distribution near permeable fault zones. The limitation of eisitization halos by the sizes of solution-supplying channels can be explained by the positive volumetric effect of mineral alterations, leading to the blockage of fractures and pores [41].

The set of metasomatic styles at the Peshchernoe deposit generally corresponds to the propylite-beresite eisite-bearing alteration type, characteristic of tectonic alteration systems. According to the model by E.V.Plyushchev et al. [43], due to the high volatility of carbon dioxide in the upper levels of the hydrothermal system, a carbonatization area can form, which corresponds to the high content of carbonates in metasomatites from the Peshchernoe deposit. A combination of beresite-listvenites and eisites in connection with mineralization is observed at the Kochkarskoe, Chudnoe, Kumakskoe and other gold deposits [44].

The study of metasomatically altered spessartites of the Peshchernoe deposit showed that Au, As, Sb, and W accumulate as a result of late sodic metasomatism. This stage is associated with a significant supply of sulphur and sulphide formation. Beresitized rocks of the Peshchernoe deposit with a superimposed association of alkaline (sodic) metasomatites have the highest gold concentrations [45]. It was the alkaline-sulphide sodium solutions that had the ore-bearing or ore-mobilizing function during gold mineralization development at the deposit. Beresitization-listvenitization created a favourable environment for ore deposition [40]. Beresitization-listvenitization, according to the metasomatic zoning theory [46], corresponds to the “felsic stage”, and eisitization may represent the “late alkaline stage”. The solubility and transport of gold in sodic hydrothermal solutions were considered by various authors [47, 48]. Recently, the possibility of extracting gold from ore using alkaline solutions of sodium polysulphide has been actively discussed [49, 50]. Gold ore deposition from alkaline solutions into relatively felsic rocks (listvenites, beresites) and quartz veins is considered in detail by V.N.Sazonov [40]. The data obtained confirm the previously identified direct relationship between mineralization related to the gold-low-sulphide-quartz formation and Ag, As, and Sb in rocks of the central segment of the East Tagil tectono-stratigraphic area, to which the Peshchernoe deposit area belongs [30].

The spatial proximity to the massif of the gabbro-diorite-granite complex, the connection of mineralization with fault zones and lamprophyre dikes, high CO_2 contents in metasomatically altered rocks, and an increased content of As, Sb, and W as a result of ore-accompanying metasomatic processes indicate that the Peshchernoe deposit can be classified as a gold prospect associated with intrusive massifs and formed in the area of their hydrothermal influence [12, 51].

Conclusion

Lamprophyres at the Peshchernoe gold deposit are represented by spessartites and kersantites. Lamprophyre dikes mark faults that later became channels for hydrothermal fluids, including ore-bearing ones. Two stages of metasomatism are distinguished in the metasomatic alterations observed in spessartites: carbon dioxide and subsequent sodic. Geochemical orientation of sodic metasomatites after spessartites indicates that it was the sodic stage of metasomatism that accompanied ore. Identification of sodic metasomatism halos in the field of widespread metasomatites of the propylite-beresite formation may be promising for more accurate localization of ore zones.

REFERENCES

1. Dirks P.H.G.M., Sanislav I.V., van Ryt M.R. et al. Chapter 8: The World-Class Gold Deposits in the Geita Greenstone Belt, Northwestern Tanzania. Geology of the World's Major Gold Deposits and Provinces. Society of Economic Geologists, 2020. Special Publication. N 23, p. 163-183. DOI: 10.5382/SP.23.08

2. Dubé B., Mercier-Langevin P., Ayer J. et al. Chapter 3: Gold Deposits of the World-Class Timmins-Porcupine Camp, Abitibi Greenstone Belt, Canada. Geology of the World's Major Gold Deposits and Provinces. Society of Economic Geologists, 2020. Special Publication. N 23, p. 53-80. DOI: 10.5382/SP.23.03

3. Mueller A.G., Hagemann S.G., McNaughton N.J. Neoarchean orogenic, magmatic and hydrothermal events in the Kalgoorlie-Kambalda area, Western Australia: constraints on gold mineralization in the Boulder Lefroy-Golden Mile fault system. *Mineralium Deposita*. 2020. Vol. 55. Iss. 4, p. 633-663. DOI: 10.1007/s00126-016-0665-9

4. Seltmann R., Goldfarb R.J., Zu B. et al. Chapter 24: Muruntau, Uzbekistan: The World's Largest Epigenetic Gold Deposit. Geology of the World's Major Gold Deposits and Provinces. Society of Economic Geologists, 2020. Special Publication. N 23, p. 497-521. DOI: 10.5382/SP.23.24

5. Goldfarb R.J., Pitcairn I. Orogenic gold: is a genetic association with magmatism realistic? *Mineralium Deposita*. 2023. Vol. 58. Iss. 1, p. 5-35. DOI: 10.1007/s00126-022-01146-8

6. Rock N.M.S., Finlayson E.J. Petrological affinities of intrusive rocks associated with the giant mesothermal gold deposit at Porgera, Papua New Guinea. *Journal of Southeast Asian Earth Sciences*. 1990. Vol. 4. Iss. 3, p. 247-257. DOI: 10.1016/S0743-9547(05)80018-2

7. Kadel-Harder I.M., Spry P.G., Layton-Matthews D. et al. Paragenetic relationships between low- and high-grade gold mineralization in the Cripple Creek Au-Te deposit, ColoraDo: Trace element studies of pyrite. *Ore Geology Reviews*. 2020. Vol. 127. N 103847. DOI: 10.1016/j.oregeorev.2020.103847

8. Kelley K.D., Jensen E.P., Rampe J.S., White D. Chapter 17: Epithermal Gold Deposits Related to Alkaline Igneous Rocks in the Cripple Creek District, Colorado, United States. Geology of the World's Major Gold Deposits and Provinces. Society of Economic Geologists, 2020. Special Publication. N 23, p. 355-373. DOI: 10.5382/SP.23.17

9. Bettles K. Chapter 13: Exploration and Geology, 1962 to 2002, at the Goldstrike Property, Carlin Trend, Nevada. Integrated Methods for Discovery: Global Exploration in the Twenty-First Century. Society of Economic Geologists, 2002. Special Publication. N 9, p. 275-298. DOI: 10.5382/SP.09.13

10. Emsbo P., Hofstra A.H., Lauha E.A. et al. Origin of High-Grade Gold Ore, Source of Ore Fluid Components, and Genesis of the Meikle and Neighboring Carlin-Type Deposits, Northern Carlin Trend, Nevada. *Economic Geology*. 2003. Vol. 98. N 6, p. 1069-1105. DOI: 10.2113/gsecongeo.98.6.1069

11. Dobak P.J., Robert F., Barker S.L.L. et al. Chapter 15: Goldstrike Gold System, North Carlin Trend, Nevada, USA. Geology of the World's Major Gold Deposits and Provinces. Society of Economic Geologists, 2020. Special Publication. N 23, p. 313-334. DOI: 10.5382/SP.23.15

12. Hart C. Reduced Intrusion-Related Gold Systems. Mineral Deposits Division. A Synthesis of Major Deposit Types, District Metallogeny, the Evolution of Geological Provinces and Exploration Methods. Geological Association of Canada, Mineral Deposits Division, 2007. Special Publication. N 5, p. 95-112.

13. Korobeinikov A.F., Gusev A.I., Krasova A.S. Reduced intrusive-alteration gold ore systems. *Izvestiya Tomskogo politekhnicheskogo universiteta*. 2012. Vol. 321. N 1, p. 16-22 (in Russian).

14. Shatova N.V., Molchanov A.V., Terekhov A.V. et al. Ryabinovoe copper-gold-porphyry stock (Southern Yakutia): geology, noble gases isotope systematics and isotopic (U-Pb, Rb-Sr, Re-Os) dating of wallrock alteration and ore-forming processes. *Regional Geology and Metallogeny*. 2019. Vol. 77, p. 75-97 (in Russian).

15. Artemiev D.S., Krymsky R.Sh., Belyatsky B.V., Ashikhmin D.S. The age of mineralization of Mayskoe gold ore deposit (Central Chukotka): results of Re-Os isotopic dating. *Journal of Mining Institute*. 2020. Vol. 243, p. 266-278. DOI: 10.31897/PMI.2020.3.266

16. Hodgson C.J., Troop D.G. A new computer-aided methodology for area selection in gold exploration; a case study from the Abitibi greenstone belt. *Economic Geology*. 1988. Vol. 83. N 5, p. 952-977. DOI: 10.2113/gsecongeo.83.5.952

17. Rock N.M.S., Groves D.I., Perring C.S., Golding S.D. Gold, Lamprophyres, and Porphyries: What Does Their Association Mean? The Geology of Gold Deposits: The Perspective in 1988. The Economic Geology Publishing Company, 1989. Economic Geology Monograph 6, p. 609-625. DOI: 10.5382/Mono.06.47

18. Rock N.M.S. Lamprophyres. New York: Springer, 1991, p. 285. DOI: 10.1007/978-1-4757-0929-2

19. Fershtater G.B., Znamenskii S.E., Borodina N.S. Age and geochemistry of the Plastovskii gold massif. *Ezhegodnik-2008. Trudy Instituta geologii i geokhimii UrO RAN*. 2009. Iss. 156, p. 276-282 (in Russian).

20. Borodaevskii N.I., Borodaevskaya M.B. Berezovskoe ore field (geological structure). Moscow: Metallurgizdat, 1947, p. 264 (in Russian).

21. Spiridonov E.M., Baksheev I.A., Filimonov S.V. Chrome spinels and genesis of pre-gold ore spessartites of the Berezovskoe ore field, Middle Urals. Magmatizm, metamorfizm i glubinnoe stroenie Urala. Tezisy dokladov VI Uralskogo petrograficheskogo soveshchaniya. V 2 tomakh. T. 2. Ekaterinburg: Institut geologii i geokhimii UrO RAN, 1997, p. 228-229 (in Russian).

22. Baksheev I.A., Belyatsky B.V. Sm-Nd and Rb-Sr isotope systems of scheelite of Berezovsky gold deposit, Middle Urals. *Lithosphere*. 2011. Vol. 4, p. 110-118 (in Russian).

23. Sazonov V.N., Murzin V.V., Grigorev N.A., Gladkovskii B.A. Endogenous mineralization of the Devonian andesitic volcano-plutonic complex (Urals). Sverdlovsk: UrO AN SSSR, 1991. 183 c (in Russian).

24. Vikentyev I.V., Tyukova E.E., Murzin V.V. et al. Vorontsovsk gold deposit. Geology, gold modes, genesis. Ekaterinburg: Fort Dialog-Iset, 2016, p. 204 (in Russian).

25. Azovskova O.B., Rovnushkin M.Yu., Soroka E.I. Petrochemical features of the dike complex of the Vorontsovskoye gold-ore deposit (Northern Urals). *News of the Ural State Mining University*. 2019. Iss. 1 (53), p. 18-27. DOI: 10.21440/2307-2091-2019-1-18-27

26. Nechkin G.S., Rovnushkin M.Yu. Sulphide near-dike mineralization at the Vorontsovskoe gold deposit (Auerbakhovskii complex, Northern Urals). *Ezhegodnik-2010. Trudy Instituta geologii i geokhimii UrO RAN*. 2011. Iss. 158, p. 187-190 (in Russian).

27. Minina O.V. Auerbakhovskii complex ore-magmatic system in the Middle Urals. *Otechestvennaya geologiya*. 1994. N 7, p. 17-23 (in Russian).

28. Ogereleva A.V., Arifulov Ch.H., Arsenteva I.V. Gold potential of Auerbakhovskii volcanic-plutonic belt (North, Subpolar, Polar Ural). *National Geology*. 2014. N 2, p. 4-19 (in Russian).

29. State Geological Map of the Russian Federation. Scale 1:200,000 (2nd generation). Seriya Sredne-Uralskaya. List O-41-I (Serov). Obyasnitelnaya zapiska. St. Petersburg: VSEGEI, 2017, p. 260 (in Russian).

30. Nesis V.N., Motov A.P., Butnyakov A.V. Geochemical characteristics and boundaries of gold ore fields of the region including Gornyachka and Peschernoe deposits, Northern Urals. *Ores and Metals*. 2020. N 1, p. 32-38 (in Russian). DOI: 10.24411/0869-5997-2020-10003

31. Puchkov V.N. Geology of the Urals and Cis-Urals (actual problems of stratigraphy, tectonics, geodynamics and metallogeny). Ufa: DesignPoligraphService, 2010, p. 280 (in Russian).

32. Hawthorne F.C., Oberti R., Harlow G.E. et al. Nomenclature of the amphibole supergroup. *American Mineralogist*. 2012. Vol. 97. N 11-12, p. 2031-2048. DOI: 10.2138/am.2012.4276

33. Bosi F., Biagioni C., Pasero M. Nomenclature and classification of the spinel supergroup. *European Journal of Mineralogy*. 2019. Vol. 31. N 1, p. 183-192. DOI: 10.1127/ejm/2019/0031-2788

34. Pasero M., Kampf A.R., Ferraris C. et al. Nomenclature of the apatite supergroup minerals. *European Journal of Mineralogy*. 2010. Vol. 22. N 2, p. 163-179. DOI: 10.1127/0935-1221/2010/0022-2022

35. Droop G.T.R. A general equation for estimating Fe^{3+} concentrations in ferromagnesian silicates and oxides from microprobe analyses, using stoichiometric criteria. *Mineralogical Magazine*. 1987. Vol. 51. Iss. 361, p. 431-435. DOI: 10.1180/minmag.1987.051.361.10

36. Azovskova O.B., Soroka E.I., Rovnushkin M.Yu., Soloshenko N.G. Sm-Nd isotopy of the dikes of the Vorontsovskoe gold-ore deposit (Northern Urals). *Vestnik of Geosciences*. 2020. N 9 (309), p. 3-6. DOI: 10.19110/geov.2020.9.1

37. Sun S.-S., McDonough W.F. Chemical and isotopic systematics of oceanic basalts: implications for mantle composition and processes. Magmatism in the Ocean Basins. London: Geological Society, 1989. Special Publication. N 42, p. 313-345. DOI: 10.1144/GSL.SP.1989.042.01.19

38. Kazitsyn Yu.V., Rudnik V.A. Guide to estimating the balance of matter and internal energy in the formation of metasomatic rocks. Moscow: Nedra, 1968, p. 364 (in Russian).

39. Zavaritskii A.N. Selected Works. In 4 volumes. Vol. 4. Moscow: Akademiya nauk SSSR, 1963, p. 727 (in Russian).

40. Sazonov V.N. Listvenitization and mineralization. Moscow: Nauka, 1975, p. 172 (in Russian).

41. Omelyanenko B.I. Wallrock hydrothermal alterations of rocks. Moscow: Nedra, 1978, p. 215 (in Russian).

42. Sazonov V.N. Gold-producing metasomatic formations of mobile belts (geodynamic settings and RTX parameters of formation, prognostic value). Ekaterinburg: Uralskaya gosudarstvennaya gorno-geologicheskaya akademiya, 1998, p. 181 (in Russian).

43. Plyushchev E.V., Shatov V.V., Kashin S.V. Metallogeny of alteration types. St. Petersburg: VSEGEI, 2012. Vol. 354, p. 560 (in Russian).

44. Sazonov V.N., Ogorodnikov V.N., Koroteev V.A., Polenov Yu.A. Gold deposits of the Urals. Ekaterinburg: Uralskaya gosudarstvennaya gorno-geologicheskaya akademiya, 2001, p. 622 (in Russian).

45. Tolochko S.A., Desyuk M.A. Geological features of the Peshchernoe gold deposit (Sverdlovsk region). Praktika geologov na proizvodstve: Sbornik trudov VII Vserossiiskoi studencheskoi nauchno-prakticheskoi konferentsii, 3 dekabrya 2022, Rostov-na-Donu, Rossiya. Rostov-na-Donu; Taganrog: Izdatelstvo Yuzhnogo federalnogo universiteta, 2022, p. 46-48 (in Russian).

46. Korzhinskii D.S. Theory of metasomatic zoning. Moscow: Nauka, 1982, p. 104 (in Russian).

47. Zvyagintsev O.E., Paulsen I.A. On the solubility of gold in alkali hydrosulphides. *Izvestiya sektora po izucheniyu platiny*. 1940. Iss. 17, p. 101-110 (in Russian).

48. Letnikov F.A., Vilor N.V. Gold in a hydrothermal process. Moscow: Nedra, 1981, p. 224 (in Russian).

49. Qingjuan Wen, Yufeng Wu, Xiu Wang et al. Researches on preparation and properties of sodium polysulphide as gold leaching agent. *Hydrometallurgy*. 2017. Vol. 171, p. 77-85. DOI: 10.1016/j.hydromet.2017.04.008

50. Sudova M., Kanuchova M., Sisol M. et al. Possibilities for the Environmental Processing of Gold-Bearing Ores. *Separations*. 2023. Vol. 10. Iss. 7. N 384. DOI: 10.3390/separations10070384

51. Baker T., Lang J.R. Fluid inclusion characteristics of intrusion-related gold mineralization, Tombstone–Tungsten magmatic belt, Yukon Territory, Canada. *Mineralium Deposita*. 2001. Vol. 36. Iss. 6, p. 563-582. DOI: 10.1007/s001260100189

***Authors*: Dmitrii V. Kuznetsov,** *Leading Engineer*, *kuznetsov@igg.uran.ru*, *https://orcid.org/0009-0003-3261-7742* (*The Zavaritsky Institute of Geology and Geochemistry of the Ural Branch of the RAS*, *Ekaterinburg*, *Russia*), **Sergei Yu. Stepanov**, *Candidate of Geological and Mineralogical Sciences*, *Senior Researcher* (*South Urals Federal Research Center of Mineralogy and Geoecology of the Urals Branch of the RAS*, *Ilmenskii State Nature Reserve*, *Miass*, *Russia*), **Andrei V. Butnyakov**, *Deputy Director* (*Ural branch of Polymetal UK*, *Yekaterinburg*, *Russia*), **Viktoriya S. Igosheva**, *Research Engineer*, *https://orcid.org/0000-0002-9158-4958* (*The Zavaritsky Institute of Geology and Geochemistry of the Ural Branch of the RAS*, *Ekaterinburg*, *Russia*).

The authors declare no conflict of interests.